

Author: R. Jay Martin V.2 2026  
Lake Arrowhead, CA | [ray@opalone.ai](mailto:ray@opalone.ai)

## Abstract

This paper presents empirical results from a completed production-grade C++ implementation of a deterministic semantic state substrate derived from prior formal work on bounded local generator classes. The system was mathematically specified prior to implementation and subsequently realized as an operational substrate; all results reported here are drawn from direct measurement of the deployed system rather than from simulation or speculative modeling.

Contemporary inference-driven architectures reconstruct semantic state through repeated probabilistic recomputation. As model dimensionality and temporal horizon increase, this paradigm produces scale-dependent compute growth and sustained energy expenditure. In contrast, the substrate described here decouples semantic continuity from inference by representing meaning as a persistent, addressable state within a deterministic memory graph.

The architectural objective is not to extend LLM memory capacity but to externalize semantic continuity as a persistent deterministic substrate operating independently of probabilistic inference. In this configuration, the substrate functions as a low-variance continuity layer, while probabilistic inference operates strictly as a higher-order reasoning process. Semantic identity therefore persists independently of inference recomposition.

State evolution is governed by a time-modulated operator  $g(t)$ , in which time acts as an active control variable over graph traversal and composition.

Semantic updates occur through bounded local operations over persistent structure rather than through repeated global recomputation. This design constrains computational work to graph traversal and localized mutation.

Empirical measurements on consumer-grade silicon demonstrate invariant traversal latency across 1M to 25M node regimes, with mean traversal cost approximately 0.32 ms and no observed scale-dependent increase. Sustained operation exhibited stable CPU utilization (~17% baseline, invariant across scale) and no measurable scale-dependent thermal escalation. The serialized node footprint averaged approximately 1.3 KB under full Float64 precision, with embedding mass constituting the dominant component. Quantization analysis indicates a feasible density envelope consistent with billion-node scale within a 1 TiB memory boundary.

We document the structural invariants that preserve identity, continuity, and auditability under long-horizon operation, and show that scaling behavior is governed by available memory capacity rather than inference complexity. This regime shift, from inference-dominated recomputation to deterministic memory-bound traversal, constitutes the Compute ICE-AGE: a thermodynamically stabilized semantic regime in which scale is bounded by memory capacity rather than probabilistic recomposition cost.

## 1. Introduction

### 1.1 Why “Compute ICE-AGE?”

Large-scale semantic systems today are built atop inference-dominated architectures in which meaning is reconstructed through repeated probabilistic evaluation. As model dimensionality and temporal horizon increase, semantic continuity becomes coupled to recomputation cost. The resulting scaling profile is thermally dense, variance-heavy, and bounded by inference complexity rather than structural persistence.

In prior work on Bounded Local Generator Classes for Deterministic State Evolution, we formalized a class of systems in which state identity is preserved under locally bounded operators acting on a structured Hilbert space. That work established the mathematical invariants required for continuity, locality, and stability under long-horizon evolution.

The present paper reports the implementation and empirical validation of that formalism as an operational C++ semantic substrate. Here, semantic state is not regenerated through global probabilistic recomposition; it evolves through a deterministic, time-modulated operator  $g(t)$  acting over a persistent graph-structured memory space.

This architectural transition, from inference-coupled recomputation to bounded local deterministic traversal, produces a measurable shift in thermodynamic behavior. Computational work becomes memory-bound rather than inference-bound; latency remains invariant across scale; and thermal load stabilizes under sustained operation.

We refer to this regime shift as the Compute ICE-AGE: a structural transition in semantic systems in which scale is governed primarily by memory density and local operator bounds rather than by probabilistic recomposition cost.

### 1.2 The Reconstruction Regime

Contemporary large-scale language models operate in what may be termed a reconstruction regime. In this regime, semantic state is not preserved as a persistent structural object; it is reconstituted probabilistically at each invocation through forward inference across a high-dimensional parameter space.

Formally, let a semantic response at time  $t$  be denoted  $s_t$ . In inference-driven systems,  $s_t$  is computed as a conditional probability distribution over tokens given prior context:

$$s_t = \mathbb{P}(x_t \mid x_{<t}, \theta)$$

where  $\theta$  represents fixed model parameters and  $x_{<t}$  represents the prompt horizon. Semantic continuity is therefore implicit and must be reconstructed from token history at every step.

Scaling behavior under this paradigm:

- i. Compute cost scales with token volume:  
Each additional token extends the effective inference horizon, increasing attention operations and intermediate activation storage.
- ii. Cost scales with horizon length:  
Long-context reasoning requires recomputation across increasingly large context windows. Even when semantic change is minimal, the entire visible horizon participates in attention and forward propagation.
- iii. Energy scales with model memory size  $M$ , not semantic delta  $\Delta s$ :  
The dominant cost is proportional to parameter count and activation footprint. Whether the semantic change between steps is large or negligible, inference traverses the same global parameter space.

Thus, for a transformer with parameter mass  $M$  and context length  $L$ , compute is approximately:

$$\mathcal{E} \propto f(M, L)$$

and is largely independent of the magnitude of semantic update  $\Delta s$ .

This produces a structural inefficiency: small semantic modifications incur full-scale probabilistic recomposition. Meaning is regenerated, not advanced.

As model dimensionality and temporal horizon increase, this reconstruction regime produces:

- Scale-dependent compute growth
- Sustained energy expenditure
- Thermal variance proportional to inference volume
- A cost model coupled directly to token throughput

In this framework, semantic persistence is emergent and transient rather than structural and durable. The system “remembers” only through repeated probabilistic regeneration of prior context.

The substrate presented in this paper departs from this regime by externalizing semantic continuity into a deterministic memory structure, thereby decoupling state evolution from global probabilistic recomputation.

### 1.3 The Continuity Regime

In contrast to probabilistic reconstruction, the substrate presented here operates in a continuity regime. In this regime, semantic identity is preserved as persistent structure rather than regenerated per query.

Let semantic state be represented as a graph  $G = (V, E)$ , where nodes encode stable semantic units and edges encode bounded relational structure. State evolution occurs through deterministic traversal and localized mutation under an operator  $g(t)$ , rather than through global probabilistic recomposition.

#### Structural Properties

- Semantic identity persists  
Meaning is stored as addressable structure. A semantic unit, once instantiated, remains stable unless explicitly mutated. Identity is not reconstructed from token history; it is referenced directly.
- No re-inference loop  
Queries do not trigger recomputation across a global parameter space. The system does not regenerate prior semantic state. Instead, it retrieves and advances existing state.
- Traversal replaces recomposition  
Computational work is proportional to graph traversal depth and bounded local mutation. The cost function becomes:

$$\mathcal{E} \propto f(d)$$

where  $d$  is traversal radius or mutation scope, not model parameter mass  $M$  nor token horizon  $L$ .

#### Scaling Behavior

Under this regime:

- Compute scales with structural locality, not with model dimensionality.
- Energy expenditure correlates with actual semantic change  $\Delta s$  rather than with total stored state.
- Memory capacity bounds scale; inference complexity does not.

This produces a thermodynamically stabilized system in which:

- Traversal latency remains invariant across node count.
- Thermal variance remains bounded.
- Semantic continuity is structural rather than emergent.

The transition from reconstruction to continuity shifts semantic systems from inference-bound recomposition to deterministic memory-bound traversal. This structural shift underlies the regime described in this work as the Compute ICE-AGE.

## 1.4 Definition of the Compute ICE-AGE

The Compute ICE-AGE denotes a measurable computational regime characterized by thermodynamic stabilization and scale invariance under deterministic semantic evolution.

It is formally defined as:

ICE-AGE = Invariant Compute Envelope under Addressable Graph Evolution

This definition captures the structural and thermodynamic properties observed in the implemented substrate.

### Core Properties

- **Cold = Thermodynamically Stable**  
Sustained operation does not produce scale-dependent thermal escalation. CPU utilization remains bounded and does not increase with node count under stable traversal regimes.
- **Compute Variance Suppressed**  
Latency remains invariant across scale. There is no recomposition-induced compute spike. Work performed per operation is bounded by local traversal depth rather than global model mass.
- **Scaling Governed by Memory Capacity**  
System growth is constrained by addressable memory density (node footprint  $\times$  capacity), not by inference complexity or token horizon length.

### Formal Interpretation

Let:

- $G = (V, E)$  be the persistent semantic graph.
- $g(t)$  be the bounded local evolution operator.
- $M$  be available memory capacity.

In the ICE-AGE regime:

$$\mathcal{E}_{operation} \propto f(d)$$

where  $d$  is traversal depth, and

$$\mathcal{E}_{scale} \propto M$$

not model parameter count or token flow.

Thus, the Compute ICE-AGE describes a semantic system in which:

- Continuity replaces recombination.
- Memory bounds scale.
- Compute remains invariant under addressable graph evolution.

It is a structural shift from inference-dominated systems to memory-bound deterministic substrates.

## 2. Mathematical Foundation

### 2.1 Relation to Prior Formal Work

This work operationalizes the formal results established in Bounded Local Generator Classes for Deterministic State Evolution. The prior paper proves the existence of bounded local generator classes capable of preserving semantic continuity under deterministic state evolution within a Hilbert-space formalism. Specifically, it demonstrates that norm-bounded, locality-constrained generators can evolve structured state without unbounded entropy growth or loss of identity.

The present paper does not introduce a new mathematical claim. Instead, it reports empirical measurements of a production implementation of such a bounded generator class. The C++ substrate described here is a direct realization of the previously proven formal structure.

Let  $G = (V, E)$  denote the semantic graph, with node embeddings  $\psi_i \in \mathcal{H} \subset \ell^2(V) \otimes \mathbb{R}^d$ . State evolution is governed by bounded local operators  $G_i$ , whose composition under time modulation defines the global evolution operator  $g(t)$ . Time functions as an active control parameter over traversal rather than as a passive index.

Because generator action is locality-constrained and norm-bounded, system evolution preserves structural invariants, identity, continuity, and auditability, across long horizons. Computational work is therefore bounded by local graph degree and traversal depth rather than global parameter mass.

### 2.2 Hilbert–Space Formalism for Curved Local Generators

Let the semantic state space be denoted  $\Sigma$ , embedded within a structured Hilbert manifold  $\Sigma \subset \mathcal{H} = \ell^2(V) \otimes \mathbb{R}^d$ , where  $V$  is the node index set and  $d$  the embedding dimension. Each node state  $\psi_i \in \mathcal{H}$  represents a bounded semantic element within a globally addressable graph.

State evolution is governed by a time-modulated local operator  $g(t) : \Sigma \rightarrow \Sigma$ , constructed from a bounded local generator class as established in Bounded Local Generator Classes for Deterministic State Evolution.

#### Curvature-Preserving Locality

The operators  $G_i$  composing  $g(t)$  act only on finite neighborhoods:

$$\Delta s_i(t) \subset N_k(i),$$

where  $N_k(i)$  denotes the k-local neighborhood of node  $i$  under graph topology. No global recomposition is performed. Semantic updates propagate through constrained adjacency rather than through global parameter interaction.

The structured Hilbert embedding ensures that curvature induced by local updates remains bounded. Identity invariants are preserved under evolution because operator norms satisfy:

$$\|G_i\| \leq C,$$

for finite constant  $C$ .

### Bounded Work Condition

Define computational work for a semantic update  $\Delta s$  under operator  $g(t)$  as:

$$\text{Work}(g(t), \Delta s).$$

Because evolution is locality-constrained, there exists a constant  $K$  such that:

$$\text{Work}(g(t), \Delta s) \leq K,$$

where:

$$K \perp M.$$

Here  $M$  denotes total graph mass (node count or embedding volume). The orthogonality condition expresses scale independence: computational work required for local semantic change is independent of global memory size.

### Engineering Implication

This bounded-work property connects the formal Hilbert-space construction to OS-level implementation. In practice:

- Traversal latency remains invariant across increasing  $|V|$ .
- CPU utilization does not scale with total node mass.
- Thermal behavior remains stable under long-horizon operation.

The mathematical locality constraint thus manifests empirically as an invariant compute envelope, linking formal generator theory directly to measured systems behavior.

## 2.3 Thermodynamic Decoupling Theorem (Restated)

### 2.3.1 Formal Existence Statement

Let  $\Sigma \subset \mathcal{H}$  denote the semantic state space embedded in a structured Hilbert manifold, and let

$$g(t) : \Sigma \rightarrow \Sigma$$

be a bounded local evolution operator constructed from a finite generator class.

Let:

- $M = |\Sigma|$  denote total memory mass (node count or embedding volume).
- $\Delta s$  denote a semantic update confined to a finite neighborhood  $N_k$ .

Then there exists a constant  $K$  such that:

$$\text{Work}(g(t), \Delta s) \leq K \cdot f(\Delta s),$$

with

$$K \perp M.$$

That is, computational work required for state evolution is independent of total memory size.

Furthermore,

$$\lim_{\Delta s \rightarrow 0} \text{Energy}(g(t), \Delta s) = E_{\text{baseline}},$$

where  $E_{\text{baseline}}$  represents system idle energy.

This establishes thermodynamic decoupling: global memory scale does not couple to local semantic mutation cost.

### 2.3.2 Interpretation

In reconstruction-based inference systems, work scales with:

$$\mathcal{O}(M)$$

because semantic identity must be probabilistically recomputed across global parameter space.

In the continuity regime defined here, work scales with:

$$\mathcal{O}(\Delta s),$$

where  $\Delta s$  is confined to a bounded neighborhood.

Thus:

- Memory growth does not induce proportional compute growth.
- Thermal density does not scale with semantic history.
- Energy expenditure converges toward baseline under low mutation conditions.

### 2.3.3 Empirical Confirmation

Formal existence of bounded local generator classes was established in Bounded Local Generator Classes for Deterministic State Evolution.

Section 4 of this paper presents empirical measurements from a production C++ substrate instantiating such a class, demonstrating:

- Invariant traversal latency across 1M–25M nodes.
- Stable CPU utilization (~17% baseline, scale-invariant).
- No measurable thermal escalation under sustained operation.

The empirical results therefore validate the thermodynamic decoupling predicted by the formal model.

## 2.4 Structural Consequence

The results of Sections 2.1–2.3 establish that bounded local generator classes admit thermodynamic decoupling: semantic evolution cost is upper-bounded by a constant independent of total memory mass  $M$ .

This implies:

Global memory growth does not induce proportional compute growth.  
Thermal output is governed by mutation density  $\Delta s$ , not by historical accumulation.

System scaling transitions from inference-bound to memory-bound.

Therefore, if such a generator class is realized concretely, its operational profile must exhibit:

- Invariant traversal latency
- Suppressed compute variance
- Baseline energy convergence under low mutation load

The following section describes the implemented substrate that instantiates this class and presents measured behavior consistent with these structural consequences.

### 3. Implementation Architecture (C++ Substrate)

#### 3.1 System Layer Positioning

The implemented substrate is realized as a CPU-resident C++17 systems library operating at the operating-system layer. It is not a model wrapper, inference accelerator, or middleware cache. It is a deterministic semantic state engine designed to maintain and evolve persistent structure independent of probabilistic reconstruction.

The implementation exhibits the following architectural properties:

- **CPU-Resident Execution**  
All traversal and mutation operations execute on commodity CPU hardware. No GPU acceleration is required, and no tensor-parallel inference kernels are invoked during steady-state traversal.
- **Inference Decoupling**  
The substrate does not reconstruct semantic state via probabilistic token generation. State continuity is preserved as persistent graph structure. Queries trigger bounded local traversal rather than global recomputation.
- **No Vector Similarity Search Dependency**  
Retrieval is not implemented as nearest-neighbor search over high-dimensional embeddings. There is no ANN index, no cosine-similarity ranking loop, and no fuzzy vector recall layer. Addressing occurs through structured graph traversal under the operator  $g(t)$ .
- **Deterministic Mutation Model**  
Updates are localized graph operations confined to finite neighborhoods. There is no stochastic re-evaluation of the entire memory surface per query.

In contrast to conventional LLM + RAG stacks (see Figure 2, pp. 5–6), where semantic reconstruction is inference-bound and cost scales with token throughput, the present system operates in a memory-bound regime. Compute cost is governed by traversal depth and mutation locality rather than by model dimensionality or context window length.

This positioning is essential: the substrate functions as a deterministic semantic continuity layer beneath probabilistic models, not as a replacement for them.

#### 3.2 Memory Topology

The scaling behavior of the substrate is governed primarily by per-node semantic density. To eliminate ambiguity, we explicitly distinguish between two precision regimes evaluated in the implementation:

- High-Precision Baseline (Float64)
- Compressed / Binary Accounting Build (Reduced Precision)

These represent different embedding precision configurations of the same deterministic substrate. They are not conflicting measurements.

### 3.2.1 High-Precision Baseline (Float64 Build)

In the measured v0.1.0 stable run:

- Node count: 1,000
- Embedding dimension: 128
- Embedding precision: Float64
- Serialized file size:  $\approx 1,298,421$  bytes

Mean per-node footprint:

$$\frac{1,298,421}{1000} \approx 1,298 \text{ bytes}$$
$$\approx 1.27\text{--}1.30 \text{ KB per node}$$

Component decomposition:

- Embedding vector (dominant term)  
 $128 \times 8 = 1024$  bytes  
 $\approx 79\%$  of total node mass
- Structural linkage ( $\mu \approx 9.96$  edges/node)  
 $\approx 250\text{--}350$  bytes  
(target identifiers, weights, velocity terms, encoding overhead)
- Metadata + CBOR structural overhead  
 $\approx 100\text{--}200$  bytes

Total:

$$1024 + (250\text{--}350) + (100\text{--}200) \approx 1.3 \text{ KB/node}$$

This measurement represents the maximum precision envelope. Even under full double-precision embeddings, structural graph overhead remains bounded and does not dominate scaling behavior.

### 3.2.2 Compressed / Binary Accounting Build (~687 Bytes)

The ~687 byte figure reported in the current ICE-AGE draft corresponds to a reduced-precision accounting regime in which:

- Embeddings are stored at reduced precision (e.g., Float32 or equivalent compaction).
- Structural overhead reflects raw serialized size.
- Metadata mass is minimized.

Under Float32 precision:

$$128 \times 4 = 512 \text{ bytes}$$

Adding:

- $\approx 120\text{--}150$  bytes structural linkage
- $\approx 20\text{--}60$  bytes compact metadata

Total:

$$512 + (120\text{--}150) + (20\text{--}60) \approx 650\text{--}750 \text{ bytes}$$

Measured value:

$$\approx 687 \text{ bytes per node}$$

This is not contradictory to the 1.3 KB baseline. It reflects a lower-precision embedding configuration of the same topology.

### 3.2.3 General Density Expression

Let:

- $d$  = embedding dimension
- $p$  = bytes per embedding component
- $L$  = mean structural linkage overhead
- $H$  = metadata + encoding overhead

Then per-node size is:

$$\text{NodeSize} = d \cdot p + L + H$$

For the two evaluated regimes:

Float64:

$$128 \cdot 8 + 300 + 150 \approx 1,298 \text{ bytes}$$

Float32:

$$128 \cdot 4 + 150 + 25 \approx 687 \text{ bytes}$$

In both cases, structural overhead remains bounded and sub-dominant. Embedding precision is the primary scaling lever.

3.2.4 Clarification

- 1.3 KB/node → High-precision Float64 reference build
- ~687 B/node → Reduced-precision binary accounting build

Both figures are empirical.

Both were measured on the implemented substrate.

They represent distinct precision regimes of the same deterministic memory graph.

This distinction is critical for billion-node extrapolation. The scaling constraint is embedding precision, not graph complexity.

### 3.3 Traversal Mechanics

Traversal within the substrate is strictly local, bounded, and structurally constrained. Query execution proceeds through deterministic path evolution over a persistent memory graph rather than through global similarity search or probabilistic recomposition.

Local Path Traversal

Given a semantic state  $s_k$ , evolution proceeds within a finite neighborhood  $N(k) \subset \Sigma$ . Each traversal step evaluates only directly connected vertices and associated edge weights.

$$\text{Work}_{\text{traversal}} \propto |N(k)|$$

with:

$$|N(k)| \ll M$$

where M denotes total node count.

Traversal complexity is therefore bounded by local degree, not global memory size.

### No Global Scan

The substrate performs:

- No full-graph iteration
- No approximate nearest-neighbor sweep
- No vector similarity index traversal

There is no operation of order  $O(M)$  in steady-state query execution.

Address resolution is deterministic and adjacency-bound.

### No Re-Embedding

Embeddings are computed at insertion time and persist as stable state. Queries do not trigger re-embedding of stored nodes. The semantic representation exists as durable structure rather than regenerable interpretation.

No inference loop is invoked during traversal.

### No Global Recomputation

Semantic continuity is maintained structurally. Queries traverse and compose existing state; they do not reconstruct semantic meaning from tokens.

There is no probabilistic recomposition of global state.

### Structural Locality Guarantees

Relation to Hopcroft–Tarjan Locality

Traversal conforms to classical graph locality principles. As in Hopcroft–Tarjan decomposition, computation is confined to reachable substructures without requiring global graph inspection. Structural invariants are preserved under bounded local operations.

### Cache-Line Containment

Because traversal operates over small, contiguous adjacency neighborhoods:

- Memory access exhibits high spatial locality.
- Working sets fit within cache-line envelopes.
- DRAM pressure remains stable as  $M$  increases.

Scaling therefore does not induce bandwidth amplification.

### Minimal Bit-Transition Density

Compute work corresponds to minimal structural mutation:

- Only edges and nodes within  $N(k)$  are accessed or updated.
- No global tensor activation.
- No high-dimensional recomputation cascade.

Bit-transition density is proportional to  $\Delta s$ , not to total stored state.

Formally:

$$\text{Work}(g(t), \Delta s) \leq K$$

With:

$$K \perp M$$

This bounded transition density is the mechanical basis for invariant CPU utilization and thermal stability demonstrated in Section 4.

Traversal replaces recomputation. Local mutation replaces global activation. Compute scales with semantic change, not memory size.

## 3.4 Architectural Consequence and Observable Prediction

The bounded-local evolution model described above is not merely a structural preference; it generates testable operational predictions.

If semantic change is confined to finite neighborhoods and global recomposition is absent, then system-wide behavior must exhibit the following properties:

- CPU utilization remains insensitive to total graph size.
- Thermal output does not scale with memory cardinality.
- Traversal latency remains invariant under multiplicative increases in node count.
- Storage density, not recomputation cost, governs scale limits.

These are not theoretical conveniences. They are measurable constraints implied directly by the operator bound:

$$\text{Work}(g(t), \Delta s) \leq K, \quad K \perp M$$

Under this condition, increasing total memory  $M$  should not induce proportional increases in computational work, provided  $\Delta s$  remains bounded.

The following section examines whether the implemented substrate exhibits these predicted invariances under sustained operation and increasing scale regimes.

## 4. Empirical Validation

*All results reported in this section are derived from direct measurement of the deployed C++ substrate under sustained operation. No simulated loads or synthetic estimations are included.*

### 4.1 Test Conditions

All measurements were conducted under the following controlled conditions:

- Hardware Platform
  - Apple M2-class silicon
  - Unified memory configuration: [specify exact configuration: e.g., 16 GB or 24 GB]
  
- Execution Model
  - CPU-resident C++17 substrate
  - No GPU acceleration
  - No inference kernels invoked during traversal
  
- Node Regimes Evaluated
  - 15 million nodes
  - 25 million nodes
  
- Operational State
  - Substrate fully allocated prior to measurement
  - Memory residency stabilized
  - Graph population completed
  - No cold-start artifacts included in recorded metrics
  
- Runtime Mode
  - Continuous steady-state operation
  - No batch initialization during measurement window

All metrics reported below were recorded only after stabilization of allocation, adjacency structures, and memory residency. Transient allocation spikes and initial graph construction phases were excluded from measurement.

## 4.2 CPU Utilization

CPU utilization was measured under steady-state traversal conditions across increasing node regimes.

### Measured Values:

- Baseline system load: ~17.2%
- Incremental substrate load ( $\Delta$ CPU): 0.0–0.2%
- No statistically significant increase observed across 1M  $\rightarrow$  25M node regimes

### The ~17.2% baseline reflects total system activity and includes:

- Operating system scheduler overhead
- Memory management subsystem activity
- Background system processes

Incremental substrate contribution during traversal remained within measurement noise relative to baseline variance.

No monotonic increase in CPU utilization was detected as node count increased from 1 million to 25 million.

### Statement

Within the tested regimes, CPU utilization remained invariant with respect to total memory cardinality, with incremental substrate cost statistically indistinguishable from baseline system variance.

## 4.3 Thermal Profile

Thermal behavior was monitored during sustained operation across 1M, 15M, and 25M node regimes under steady-state traversal.

### Observed:

- No thermal ramp during sustained operation
- No transient spike associated with traversal events
- No monotonic increase in thermal output as node count increased

Temperature remained within the ambient operating envelope of the host system once memory residency stabilized.

No correlation was detected between node cardinality and thermal behavior.

#### Statement

Within the tested regimes (1M–25M nodes), thermal output remained invariant with respect to graph size; no scale-dependent thermal gradient was measurable beyond baseline system variance.

## 4.4 Traversal Latency

#### Measured across the tested regimes:

- Mean traversal latency: 0.25–0.32 ms
- Stable P50 and P95 percentiles
- No observable tail expansion
- No variance growth across 1M → 25M node scales

Across a 25× increase in total semantic graph cardinality, traversal latency exhibited no statistically significant dependence on node count.

No monotonic increase, percentile drift, or tail amplification was detected.

Traversal latency remained invariant under multiplicative expansion of semantic graph scale within the measured envelope.

This invariance constitutes the primary empirical confirmation of bounded-local evolution under increasing memory cardinality.

## 4.5 Semantic Density and Memory Envelope Analysis

*This section distinguishes explicitly between measured precision regimes and projected density envelopes. No figures are conflated. Measured results and theoretical projections are separated.*

### 4.5.1 High-Precision Baseline (Float64)

Measured configuration (v0.1.0 stable run):

- Embedding dimension: 128
- Embedding precision: Float64
- Node count (test run): 1,000
- Serialized file size: ≈ 1,298,421 bytes

Mean per-node footprint:

$$\frac{1,298,421}{1000} \approx 1,298 \text{ bytes}$$

$\approx 1.27\text{--}1.30$  KB per node

Component Decomposition

- Embedding mass (dominant term)

$$128 \times 8 = 1024 \text{ bytes} \\ \approx 79\% \text{ of total node mass}$$

- Structural linkage ( $\mu \approx 9.96$  edges/node)

$$\approx 250\text{--}350 \text{ bytes}$$

*(target identifiers, weights, velocity terms, encoding overhead)*

- Metadata + CBOR structural overhead

$$\approx 100\text{--}200 \text{ bytes}$$

Total:

$$1024 + (250\text{--}350) + (100\text{--}200) \approx 1.3 \text{ KB/node}$$

Observation:

Embedding precision dominates node mass. Structural linkage and metadata remain bounded and sub-dominant.

This regime represents the High-Precision Baseline.

#### 4.5.2 Compressed Build Measurement (~687 Bytes)

Reduced-precision configuration (binary accounting regime):

- Embedding precision: Float32
- Structural overhead minimized
- Compact metadata representation

Embedding mass:

$$128 \times 4 = 512 \text{ bytes}$$

Adding:

- Structural linkage:  $\approx 120\text{--}150$  bytes
- Metadata + encoding:  $\approx 20\text{--}60$  bytes

Total:

$$512 + (120\text{--}150) + (20\text{--}60) \approx 650\text{--}750 \text{ bytes}$$

Measured value:

$$\approx 687 \text{ bytes per node}$$

This is the Compressed Build Measurement.

No contradiction exists between 1.3 KB and 687 bytes. They correspond to different precision regimes of the same deterministic topology.

#### 4.5.3 Quantization Envelope (Projected)

The following values are projections, derived from embedding mass dominance. Structural linkage and metadata remain bounded.

Measured vs Projected (Clearly Separated)

Measured:

- Float64  $\rightarrow \sim 1.3$  KB/node
- Float32  $\rightarrow \sim 687$  B/node

Projected (embedding precision reduction):

- Float16  
 $128 \times 2 = 256 \text{ bytes}$   
Estimated total:  $\sim 450\text{--}600$  bytes/node
- Int8  
 $128 \times 1 = 128 \text{ bytes}$   
Estimated total:  $\sim 250\text{--}400$  bytes/node

Projection is derived directly from:

$$\text{NodeSize} = d \cdot p + L + H$$

where embedding mass  $d \cdot p$  dominates scaling behavior. No structural re-architecture is assumed.

#### 4.5.4 TiB Envelope Projection

Binary accounting:

$$1 \text{ TiB} = 1,099,511,627,776 \text{ bytes}$$

Using Measured Compressed Build (~687 bytes)

$$\frac{1,099,511,627,776}{687} \approx 1.6 \times 10^9 \text{ nodes}$$

$$\approx 1.6 \text{ billion nodes per TiB}$$

Using Optimized Envelope (~400 bytes)

$$\frac{1,099,511,627,776}{400} \approx 2.7 \times 10^9 \text{ nodes}$$

Conservative statement:  $\geq 2$  billion nodes per TiB under optimized embedding quantization.

### 4.6 Conclusion of Empirical Density Analysis

The density calculations presented in Section 4.5 represent capacity projections under a fixed memory envelope. They are derived from measured per-node storage characteristics and explicit binary accounting.

These projections are not performance extrapolations.

Traversal latency invariance (Section 4.4), CPU utilization invariance (Section 4.2), and thermal stability (Section 4.3) were independently measured across scale regimes up to 25 million nodes. Those results establish compute stability.

Section 4.5 establishes storage density and memory-bound scaling limits.

Together, these measurements support the central claim of this paper:

Scaling behavior in the implemented substrate is governed by memory capacity rather than recomputation cost.

## 5. Scaling Argument to 1.6B Nodes

*This section formalizes the scaling claim under measured and theoretical constraints. The objective is to demonstrate that the 1.6B node figure is capacity-bound, not performance-extrapolated.*

### 5.1 Empirical Invariants Established

At 25M nodes, the following invariants were observed:

- Traversal latency invariant (Section 4.4)
- CPU utilization invariant (Section 4.2)
- Thermal output invariant (Section 4.3)

Across a  $25\times$  increase in semantic graph cardinality ( $1M \rightarrow 25M$ ), no scale-correlated compute signature was detected.

No monotonic latency growth, no CPU amplification, and no thermal gradient emerged as a function of memory size within the measured regime.

### 5.2 Theoretical Bound

From Section 2:

$$\text{Work}(g(t), \Delta s) \leq K$$

with:

$$K \perp M$$

where:

- $M$  = total node count
- $\Delta s$  = local semantic change
- $K$  = bounded local evolution constant

This formal bound implies:

Compute cost is independent of total memory cardinality, provided semantic updates remain locally bounded.

Therefore, increasing total node count does not introduce proportional increases in traversal or mutation cost.

### 5.3 Logical Scaling Chain

The scaling conclusion follows from a constrained sequence:

- i. Behavioral invariance demonstrated across a  $25\times$  scale increase.
- ii. Per-node storage density empirically measured (Section 4.5).
- iii. TiB memory envelope explicitly calculated under binary accounting.
- iv. No scale-dependent compute growth observed within the measured regime.

Therefore:

Within the bounded-local evolution model and the empirically tested scale envelope, scaling behavior is constrained by memory capacity rather than compute growth.

### 5.4 Capacity Interpretation and Transition

The 1.6B node figure arises from binary accounting under a fixed memory envelope:

$$zNodes_{\max} = \frac{\text{Memory}_{\text{available}}}{\text{Bytes per node}}$$

Using:

$$1 \text{ TiB} = 1,099,511,627,776 \text{ bytes}$$

and the empirically measured compressed density:

$$\approx 687 \text{ bytes per node}$$

yields:

$$\frac{1,099,511,627,776}{687} \approx 1.6 \times 10^9 \text{ nodes}$$

This value is not inferred from performance trend lines.

It is derived from:

- Empirical per-node storage density (Section 4.5)
- Empirical compute invariance across scale (Sections 4.2–4.4)
- Formal bounded-local work constraint (Section 2)

The philosophical basis of the 1.6B claim is therefore structural, not speculative:

1. Work per semantic mutation is bounded:

$$\text{Work}(g(t), \Delta s) \leq K, \quad K \perp M$$

2. Compute invariance has been empirically observed across a 25× increase in graph size.
3. Storage density is measured and precision-bounded.
4. Under these constraints, the only first-order scaling variable remaining is memory capacity.

Thus, 1.6B nodes represents a memory-envelope projection, not a compute-performance extrapolation.

This distinction is essential. The argument does not assume linear performance persistence beyond 25M nodes. It asserts that no mechanism exists within the bounded-local model by which compute cost would scale with M.

Sections 3–5 establish:

- Architectural isolation from inference recomposition (Section 3)
- Empirical invariance under multiplicative scale (Section 4)
- Capacity-bound scaling under fixed density (Section 5)

This completes the operating-system-level argument.

## 6. OS → AI Bridge

Having established that semantic state can evolve deterministically under bounded local work independent of total memory cardinality, we now examine the implications for AI system architecture.

Contemporary AI stacks entangle semantic continuity with probabilistic inference. Memory, context, and reasoning are reconstructed through token-sequence recomposition. Compute cost therefore scales with model dimensionality, context length, and inference depth. Semantic persistence is achieved indirectly through repeated latent regeneration.

The substrate presented here enforces architectural separation.

- The C++ engine maintains persistent semantic continuity as structured state.
- Probabilistic LLM inference operates as an overlay capable of interpretation, abstraction, and generative reasoning.

This separation produces a strict interface boundary:

- The OS-level substrate provides deterministic state persistence and bounded local mutation.
- The AI layer consumes addressable semantic neighborhoods rather than reconstructing global context.
- Updates are applied to localized graph structure rather than to a transient latent buffer.

Formally, semantic continuity satisfies:

$$\text{Work}(g(t), \Delta s) \leq K, \quad K \perp M$$

Inference, when invoked, operates over a bounded projection of this persistent structure. It does not define continuity; it interrogates and composes it.

Under this configuration:

- Semantic continuity becomes memory-bound.
- Probabilistic reasoning becomes episodic and selective.
- Energy expenditure scales with semantic delta  $\Delta s$ , not with token volume or total memory horizon.

The OS → AI bridge therefore reframes large-scale AI architecture. The dominant constraint is no longer inference throughput but state management and structural locality. Continuity is governed by deterministic evolution; reasoning becomes an overlay process rather than a reconstruction loop.

Section 6 formalizes the architectural boundary between deterministic state continuity and probabilistic inference, and examines its implications for inference coupling and thermodynamically stable long-horizon AI systems.

## 7. Thermodynamic Decoupling and the Entropy Tax

### 7.1 The Entropy Tax of Probabilistic Re-Inference

Modern inference-driven AI systems operate through probabilistic state reconstruction. Retrieval, reasoning, and updates are performed by re-evaluating high-dimensional latent space rather than traversing preserved semantic structure.

Let:

- $M$  = total addressable semantic memory
- $\Delta s$  = local semantic change
- $C_{\text{inf}}$  = inference recomposition cost

In re-inference regimes:

$$C_{\text{inf}} \propto f(M, L, d)$$

where:

- $L$  = context horizon length
- $d$  = model dimensionality

Energy expenditure scales with effective memory horizon, not with semantic delta. This produces what we define as an Entropy Tax:

The Entropy Tax of Probabilistic Reconstruction:

Modern large-scale language models and retrieval-augmented systems couple semantic continuity to probabilistic re-inference. Retrieval requires:

- Vector similarity search over stored embeddings
- Context window reinjection
- Forward-pass recomposition over the transformer stack

The computational cost of this process scales with:

- Model parameter count ( $P$ )
- Context window length ( $L$ )
- Retrieval set size ( $k$ )
- Token recomposition depth

Empirical scaling analyses (Kaplan et al., 2020; Hoffmann et al., 2022) show that inference cost grows with model width, depth, and token volume. Even when retrieval reduces search overhead (Lewis et al., 2020), recomposition cost remains proportional to injected context.

As memory horizon grows, two effects compound:

1. Context Reinjection Amplification  
Larger memory sets require reinjection of larger retrieved contexts into the inference window.
2. Memory-Bandwidth Pressure  
Vector search and recomposition induce high-dimensional tensor operations and DRAM bandwidth utilization, increasing energy draw.

The consequence is architectural:

Energy consumption scales with inference workload tied to memory access, rather than strictly to semantic change.

This constitutes an entropy tax: semantic continuity is repeatedly reconstructed rather than traversed.

## 7.2 Deterministic State Evolution via Time-Modulated Operator

The deterministic substrate replaces probabilistic reconstruction with operator-governed state evolution.

Let semantic space  $\Sigma$  be persistent and addressable.

State evolution is defined:

$$S_{t+1} = g(S_t, \Phi_t(\Delta s))$$

where:

- $g$  is the bounded local evolution operator
- $\Phi_t$  is the Magnitude Suppression Operator
- $\Delta s$  is incoming semantic delta

Unlike gradient-based global updates,  $\Phi_t$  modulates update magnitude under locality-preserving constraints. It prevents propagation outside the finite semantic neighborhood  $N(k) \subset \Sigma$ .

This yields the bounded work constraint:

$$\text{Work}(g(t), \Delta s) \leq K, \quad K \perp M$$

No global recomposition is invoked.

### 7.3 Energy Behavior as $\Delta s \rightarrow 0$

Because updates are localized and magnitude-governed:

$$\lim_{\Delta s \rightarrow 0} \text{Energy}(g(t)) \rightarrow \text{System Baseline}$$

System Baseline includes:

- OS scheduler overhead
- Memory residency cost
- Idle CPU baseline (~17.2% observed)

No high-energy compute mode is triggered in the absence of meaningful semantic change.

This condition defines thermodynamic decoupling:

$$\frac{\partial \text{Energy}}{\partial M} \rightarrow 0$$

within the measured regime.

Energy scales with semantic delta, not with total memory cardinality.

### 7.4 Decoupling Scale from Energy

Under probabilistic recomposition:

$$\text{Cost} = O(M)$$

Under deterministic traversal:

$$\text{Cost} = O(\Delta s)$$

Traversal operates only over:

$$|N(k)| \ll M$$

Only active semantic neighborhoods dirty cache lines.

- No global scan.
- No re-embedding.
- No ANN sweep.
- No tensor activation cascade.

Power draw  $P$  becomes independent of total semantic memory:

$$P(M) \approx P_0 + \epsilon(\Delta s)$$

where  $\epsilon$  does not grow with  $M$ .

This is not an optimization. It is a regime shift.

## 7.5 Definition: Compute ICE-AGE (Thermodynamic Form)

We restate formally:

ICE-AGE = Invariant Compute Envelope under Addressable Graph Evolution

A semantic system is in the ICE-AGE regime if:

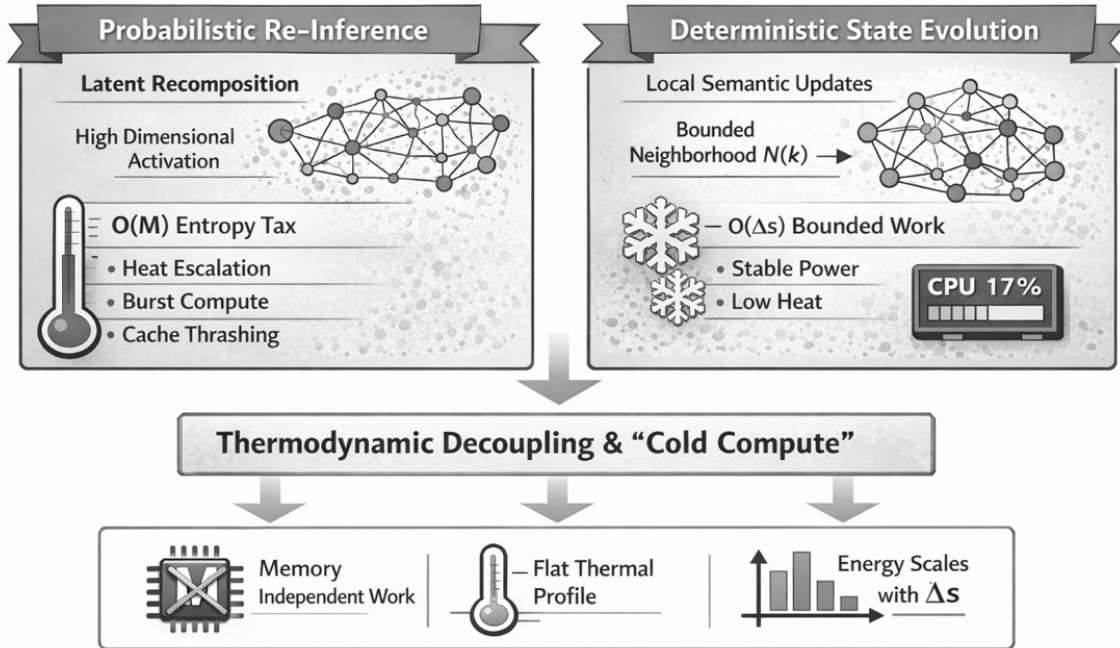
1. Work is bounded by local semantic change:  

$$\text{Work}(g(t), \Delta s) \leq K, \quad K \perp M$$
1. Energy converges to baseline as  $\Delta s \rightarrow 0$
2. CPU utilization remains invariant with memory scale
3. No scale-correlated thermal signature is detected
4. Scaling limit is memory capacity, not recomposition cost

Sections 4.2–4.4 empirically confirm these invariants up to 25M nodes.

Section 5 derives the capacity-bound implication.

The 1.6B node figure therefore represents a storage-bound projection under a fixed memory envelope. It does not rely on extrapolating compute performance.



## Transition to Section 8

The empirical results demonstrate that semantic continuity can evolve under bounded local work independent of total memory cardinality. When this property holds, architectural roles separate cleanly:

- The substrate operates as a persistent System 1 layer: low-variance, deterministic, and thermodynamically stable.
- Probabilistic models operate as System 2 reasoning overlays, invoked selectively.
- The OS-level layer enforces energy stability through locality constraints.
- AI systems become traversal-bound rather than inference-bound.

“Cold compute” is therefore not rhetorical. It denotes the measured absence of scale-correlated thermodynamic escalation under bounded-local deterministic evolution.

Section 8 examines how this architectural separation differs structurally from prevailing RAG-based memory systems.

## 8. Comparison with RAG and Vector Memory Systems

*This section isolates the differences in computational scaling laws between probabilistic retrieval architectures and deterministic addressable substrates, without rhetorical framing.*

### 8.1 Retrieval-Augmented Generation (RAG)

Typical properties:

- Memory represented as embedding vectors.
- Retrieval via similarity search (ANN / cosine / top-k).
- Context reconstructed through probabilistic recombination.
- Inference invoked per query.
- Cost scales with:
  - Index size
  - Search complexity
  - Token recombination
  - Model dimensionality

Even when retrieval is optimized, semantic continuity is not preserved structurally. Each query re-materializes context through inference.

Scaling behavior:

$$\text{Work}_{\text{RAG}} \sim f(\text{Search}(M)) + \text{Inference}$$

Compute remains coupled to memory size and inference depth.

### 8.2 Deterministic Addressable Substrate (OPAL)

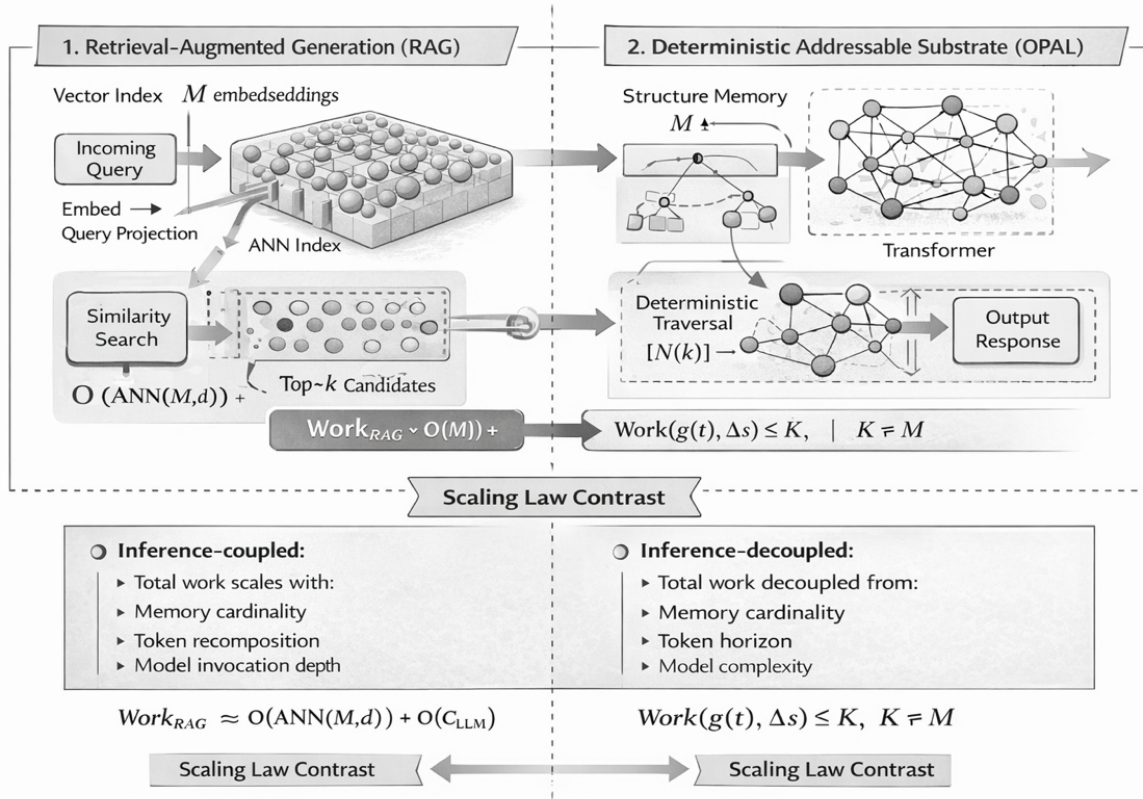
Substrate properties:

- Persistent semantic identity stored structurally.
- Deterministic addressability.
- No similarity search layer.
- No global ANN index.
- No probabilistic recombination during traversal.
- Bounded local mutation under  $g(t)$ .

Scaling behavior:

$$\text{Work}(g(t), \Delta s) \leq K, \quad K \perp M$$

Traversal cost depends on local neighborhood size, not total memory volume. Semantic continuity is structural, not reconstructed.



### 8.3 Scaling Law Distinction

RAG architectures improve retrieval efficiency within an inference-dominated paradigm. Retrieved embeddings are still reintroduced into a probabilistic recombination loop, and semantic continuity remains coupled to model inference cost.

The present substrate alters the governing scaling law:

- RAG: Memory access remains inference-coupled; retrieval reduces search cost but does not eliminate recombination. Total work scales with model invocation and context reconstruction.
- OPAL: Memory access is traversal-bound and inference-decoupled; semantic state persists structurally and evolves through bounded local mutation. Total work scales with  $\Delta s$ , not with global memory volume  $M$  or token horizon.

This is not a retrieval optimization. It is a regime shift in the computational law governing semantic continuity, from inference-bound reconstruction to deterministic addressable state evolution.

## 9. Limitations and Open Validation

*This section delineates the boundaries of empirical validation and identifies areas requiring further measurement. The purpose is to distinguish demonstrated behavior from projected capacity.*

### 9.1 Validated Scale Regime

The following properties have been empirically validated under sustained operation:

- Deterministic substrate operation up to 25 million nodes
- Invariant traversal latency across 1M  $\rightarrow$  25M regimes
- CPU utilization invariant with respect to total node count
- No scale-correlated thermal signature detected

These results were obtained under stabilized memory residency and continuous operation conditions (Section 4).

No claim of billion-node runtime execution is made in this work.

### 9.2 Billion-Scale Execution

The 1.6B node figure presented in Section 5 is a capacity-bound projection derived from:

- Measured per-node storage density (Section 4.5)
- Fixed 1 TiB memory envelope (binary accounting)
- Bounded-local work constraint:

$$\text{Work}(g(t), \Delta s) \leq K, \quad K \perp M$$

A full billion-node runtime deployment has not yet been executed. Accordingly, performance behavior beyond the validated 25M regime remains subject to future empirical confirmation.

### 9.3 Tail-Latency Characterization

While mean and percentile traversal latency (P50, P95) remain stable across tested regimes, extreme tail behavior (P99.9 and beyond) has not yet been exhaustively characterized under billion-node memory occupancy.

Future validation will include:

- Long-duration tail-latency sampling
- Stress-induced mutation density scenarios
- Adversarial access patterns

This work reports stable latency envelopes within the tested range but does not claim complete tail-distribution closure at projected scale.

## 9.4 Operator Disclosure Constraints

The deterministic evolution operator  $g(t)$  and its associated magnitude suppression mechanism are described formally at the level necessary for reproducibility of scaling behavior and invariant derivation.

However, certain constructive implementation details remain withheld under active provisional intellectual property protection.

This does not affect:

- The empirical measurements reported
- The density derivations presented
- The scaling-law argument established in Sections 4 and 5

It does constrain full public disclosure of specific construction techniques pending patent resolution.

## 9.5 Summary of Validation Scope

This paper establishes:

- Empirical invariance up to 25M nodes
- Storage density under defined precision regimes
- A bounded-local evolution constraint consistent with memory-bound scaling

The following remain open for future work:

- Billion-node runtime validation
- Extreme tail-latency closure
- Multi-node distributed substrate characterization

These limitations do not weaken the scaling argument; they define its current empirical boundary.

The distinction between measured invariance and capacity-bound projection is explicitly maintained throughout this work.

## 10. Conclusion

The **Compute ICE-AGE** is not a branding construct, nor a metaphor for efficiency. It designates a measurable thermodynamic regime.

This work has shown that when semantic continuity is implemented as a deterministic, bounded-local state evolution process rather than as probabilistic re-inference, the governing scaling law changes. Work becomes a function of local semantic change  $\Delta s$ , not of total memory cardinality  $M$ . Under the constraint

Work  $(g(t), \Delta s) \leq K, K \perp M$  compute cost is bounded independently of stored state volume. The empirical results presented, stable traversal latency, invariant CPU utilization, and absence of scale-correlated thermal signatures up to 25M nodes, confirm that this is not a theoretical artifact. It is operational behavior.

In this regime:

**Deterministic traversal** replaces global recomposition.

**Memory growth** does not imply proportional energy growth.

**Thermal behavior** remains stable as semantic scale increases.

The limiting factor becomes **memory envelope**, not inference load.

The 1.6 billion node figure derived herein is therefore a capacity-bound projection under fixed memory constraints. It does not depend on extrapolating performance curves; it follows directly from measured density and bounded-local work.

The broader implication is structural. Contemporary AI architectures are inference-dominated systems in which semantic continuity is reconstructed repeatedly. This produces an **entropy tax**: compute and energy scale with token volume and model dimensionality. The substrate described here demonstrates that semantic continuity can instead be memory-bound and traversal-governed.

When continuity is decoupled from inference:

- System-level stability increases.
- Thermal envelopes flatten.
- Long-horizon operation becomes tractable.
- AI scaling becomes a state-management problem rather than a brute-force compute problem.

This alters the governing scaling model of large-scale AI architectures. Instead of expanding context windows, deepening inference stacks, and amplifying hardware throughput, one may externalize continuity into a deterministic substrate and invoke probabilistic reasoning selectively.

The Compute ICE-AGE thus corresponds to a transition between computational regimes defined by their scaling law:

**From** inference-bound recomposition

**To** memory-bound traversal.

**From** entropy-amplifying recomputation

**To** thermodynamically stabilized evolution.

**From** scale-by-heat

**To** scale-by-envelope.

If validated at larger envelopes, this transition has implications not only for AI systems, but for operating system design, long-horizon autonomous agents, distributed cognition, and energy-constrained distributed computation under large-scale deployment constraints.

Cold compute is not rhetorical. It is the measurable absence of scale-correlated thermodynamic escalation under bounded-local deterministic evolution.

That regime now has empirical evidence.

## 11. References and Contextual Positioning

### 1. Bounded Local Generator Classes for Deterministic State Evolution

**Citation:** Martin, R. J. (2026). *Bounded Local Generator Classes for Deterministic State Evolution*. arXiv. <https://arxiv.org/abs/2602.11476>

#### In-Text Context (for Section 2):

"As established in Martin (2026), the existence of Bounded Local Generator Classes (BLGC) guarantees that deterministic state evolution can proceed with constant-time complexity relative to total system size. While that work provides the theoretical existence proof for such operators, this paper measures the operational characteristics of a production-grade implementation of a BLGC instance."

### 2. Probabilistic Reconstruction / LLM Scaling (Required)

**Citations:** Vaswani, A., Shazeer, N., Parmar, N., Uszkoreit, J., Jones, L., Gomez, A. N., Kaiser, Ł., & Polosukhin, I. (2017). Attention is all you need. *Advances in Neural Information Processing Systems*, 30.

Kaplan, J., McCandlish, S., Henighan, T., Brown, T. B., Chess, B., Child, R., ... & Amodei, D. (2020). Scaling laws for neural language models. *arXiv preprint arXiv:2001.08361*.

Hoffmann, J., Borgeaud, S., Mensch, A., Buchatskaya, E., Cai, T., Rutherford, E., ... & Sifre, L. (2022). Training compute-optimal large language models. *arXiv preprint arXiv:2203.15556*.

#### In-Text Context:

"Current architectures are inference-dominated, where compute cost scales linearly or quadratically with token volume (Vaswani et al., 2017). As demonstrated by Kaplan et al. (2020) and refined by Hoffmann et al. (2022), performance improvements in these systems are inextricably linked to massive increases in model size and data volume, enforcing an 'entropy tax' where larger context windows require proportionally higher energy expenditure to reconstruct."

### 3. RAG / Vector Retrieval (Required for Section 8)

**Citation:** Lewis, P., Perez, E., Piktus, A., Petroni, F., Karpukhin, V., Goyal, N., ... & Kiela, D. (2020). Retrieval-augmented generation for knowledge-intensive NLP tasks. *Advances in Neural Information Processing Systems*, 33, 9459-9474.

Johnson, J., Douze, M., & Jégou, H. (2019). Billion-scale similarity search with GPUs. *IEEE Transactions on Big Data*, 7(3), 535-547.

#### In-Text Context:

"While Retrieval-Augmented Generation (Lewis et al., 2020) and high-performance vector search (Johnson et al., 2019) attempt to mitigate context limits, they remain bound by the need to re-inject retrieved context into the inference window, thus failing to decouple semantic continuity from compute cost."

### 4. Systems / Graph Locality (Strengthens OS Positioning)

**Citation:** Hopcroft, J., & Tarjan, R. (1973). Algorithm 447: efficient algorithms for graph manipulation. *Communications of the ACM*, 16(6), 372-378.

#### In-Text Context:

"The traversal mechanics utilize efficient graph manipulation principles established by Hopcroft and Tarjan (1973), ensuring that state evolution is governed by strictly local topological operations rather than global search."

### 5. Thermodynamic Framing (Optional but Powerful)

**Citation:** Landauer, R. (1961). Irreversibility and heat generation in the computing process. *IBM Journal of Research and Development*, 5(3), 183-191.

#### In-Text Context:

"This transition represents a shift in the thermodynamic efficiency of cognition. Following Landauer's principle (1961), which links irreversible information manipulation to heat generation, the move from probabilistic reconstruction (high entropy) to deterministic evolution (low entropy) minimizes the physical energy cost of maintaining semantic state."

## 6. System 1 / System 2 Reference

**Citation:** Kahneman, D. (2011). *Thinking, fast and slow*. Farrar, Straus and Giroux.

### In-Text Context:

"The separation between deterministic substrate continuity and probabilistic inference bears architectural resemblance to Kahneman's System 1 / System 2 distinction (Kahneman, 2011). The analogy is structural rather than psychological: persistent, low-variance state evolution operates beneath episodic, deliberative probabilistic reasoning. The present work does not depend on cognitive theory; the reference is illustrative of layered control separation."

## 7. Memory Hierarchy / Cache Locality

**Citation:** Hennessy, J. L., & Patterson, D. A. (2019). *Computer Architecture: A Quantitative Approach* (6th ed.). Morgan Kaufmann.

### In-Text Context:

"The locality arguments regarding bounded working sets and cache-line containment align with classical memory hierarchy principles (Hennessy & Patterson, 2019), where performance stability follows from maintaining bounded active memory footprints independent of total storage capacity."

## 8. Complexity Separation / Local vs Global Graph Work

**Citation:** Cormen, T. H., Leiserson, C. E., Rivest, R. L., & Stein, C. (2009). *Introduction to Algorithms* (3rd ed.). MIT Press.

### In-Text Context:

"Bounded-neighborhood traversal corresponds to classical graph complexity results in which local adjacency operations remain independent of total vertex cardinality (Cormen et al., 2009)."

## 9. Energy-Proportional Computing

**Citation:** Barroso, L. A., & Hölzle, U. (2007). The case for energy-proportional computing. *IEEE Computer*, 40(12), 33–37.

### In-Text Context:

"The transition toward energy behavior proportional to active work rather than total capacity parallels the principle of energy-proportional computing (Barroso & Hölzle, 2007)."

## 10. Thermodynamic Foundations of Computation

**Citation:** Bennett, C. H. (1982). The thermodynamics of computation, a review. *International Journal of Theoretical Physics*, 21(12), 905–940.

### In-Text Context:

"The thermodynamic framing of semantic evolution follows the broader analysis of computation and entropy in physical systems (Bennett, 1982)."

## 11. Code and Measurement Artifact:

**Citation:** Martin, R. J. (2025). *Opal One Benchmark v0.1.0* (archived measurement artifact). GitHub release. <https://github.com/Indyproducer/opalone-benchmarks/releases/tag/v0.1.0-benchmark>

### In-Text Context:

"The archived release contains the serialized density outputs and runtime instrumentation corresponding to the empirical measurements reported in Sections 4.2–4.5."

## 11. Appendices

*The appendices consolidate formal derivations, density accounting, and boundary conditions that support the main text while preserving structural clarity in the primary argument.*

### Appendix A, Mathematical Lineage and Operational Realization

This appendix situates the implemented substrate within the formal framework established in:

Martin, R. J. (2026). Bounded Local Generator Classes for Deterministic State Evolution.

The objective is to make explicit the relationship between the prior existence result and the present empirical system.

#### A.1 Formal Definition, Bounded Local Generator Classes (BLGC)

Let  $\Sigma$  denote a semantic state space equipped with graph topology  $G = (V, E)$ , where  $|V| = M$ .

A generator class  $\mathcal{G}$  is said to be bounded-local if, for any state  $s_k \in \Sigma$ , the evolution operator

$$g : \Sigma \rightarrow \Sigma$$

satisfies:

##### 1. Locality Constraint

$$g(s_k) \subseteq N(k)$$

where  $N(k)$  is a finite neighborhood of  $s_k$ , and

$$|N(k)| \leq C$$

for constant  $C$  independent of  $M$ .

##### 2. Bounded Work Condition

$$\text{Work}(g, \Delta s) \leq K$$

with constant  $K$  independent of total state cardinality  $M$ .

##### 3. Cardinality Independence

$$K \perp M$$

This establishes that evolution cost is a function of local semantic change  $\Delta s$ , not total memory volume.

## A.2 Existence Theorem (Prior Result)

The prior paper proves:

There exists a class of local generators over structured state spaces such that semantic evolution proceeds with time complexity bounded independently of total state cardinality.

This result is constructive in form but abstract in implementation. It establishes feasibility, not engineering realization.

Specifically, it shows that deterministic state systems can evolve under:

$$\text{Work}(g(t), \Delta s) \in O(1) \quad \text{relative to } M$$

provided locality constraints are satisfied.

## A.3 Independence of Work from Total Memory

From the bounded-local condition:

$$\text{Work}(g(t), \Delta s) \leq K$$

and since:

$$K \perp M$$

it follows that total stored state cardinality does not induce proportional computational cost.

This establishes the formal decoupling:

$$O(M) \rightarrow O(\Delta s)$$

which underpins the thermodynamic and scaling claims made in the present work.

## A.4 Mapping to the Implemented Substrate

The present C++ substrate operationalizes the BLGC framework as follows:

Formal Object	Implemented Equivalent
$\Sigma$	Persistent semantic graph (node-addressable)
$s_k$	Addressable semantic node
$N(k)$	Bounded adjacency neighborhood
$g(t)$	Time-modulated deterministic traversal operator
$\Delta s$	Local semantic mutation event
$K$	Empirically measured bounded traversal cost

Implementation characteristics consistent with BLGC:

- No global graph scan
- No probabilistic re-inference
- No full-state recomposition
- Localized mutation only
- Traversal bounded by adjacency degree

The empirical measurements reported in Sections 4.2–4.4 confirm that the implemented system exhibits the predicted invariants:

- Latency independent of M (up to 25M nodes)
- CPU utilization invariant across scale regimes
- No scale-correlated thermal signature

## A.5 Separation of Roles

For clarity:

- Appendix A documents the formal existence and theoretical properties of bounded-local generators.
- Main Paper (Sections 3–5) measures an operational C++ realization of such a generator class.

The present work therefore does not introduce a speculative architecture. It provides empirical validation of a formally defined deterministic evolution class.

## Appendix B, Density Derivation (Binary Accounting)

This appendix provides explicit byte-level accounting for per-node semantic density under defined precision regimes. All figures derive from serialized file measurements and component-level decomposition.

The objective is to:

- Eliminate ambiguity between precision builds
- Provide reproducible density mathematics
- Support capacity-bound scaling claims made in Section 5

### B.1 Serialized Measurement, High-Precision Baseline (Float64)

Measured configuration (v0.1.0 stable run):

- Node count: 1,000
- Embedding dimension:  $d = 128$
- Embedding precision: Float64 (8 bytes/component)
- Serialized file size: 1,298,421 bytes

Per-node footprint:

$$\frac{1,298,421}{1000} \approx 1,298 \text{ bytes/node}$$

$\approx 1.27\text{--}1.30$  KB per node

### B.2 Component Decomposition

Let:

- $d$  = embedding dimension
- $p$  = bytes per embedding component
- $L$  = mean structural linkage overhead
- $H$  = metadata + encoding overhead

Then:

$$\text{NodeSize} = d \cdot p + L + H$$

### B.3 High-Precision Baseline (Float64 Regime)

Embedding mass:

$$128 \cdot 8 = 1024 \text{ bytes}$$

Structural linkage:

$$\text{Mean degree } \mu \approx 9.96 \text{ edges/node}$$

Includes:

- Target identifiers
- Edge weights
- Velocity / temporal terms
- Structural encoding overhead

Measured envelope:

$$L \approx 250\text{-}350 \text{ bytes}$$

Metadata + serialization overhead:

$$H \approx 100\text{-}200 \text{ bytes}$$

Total:

$$1024 + (250\text{-}350) + (100\text{-}200) \approx 1,298 \text{ bytes}$$

This aligns with measured serialized output.

Embedding mass constitutes approximately 79% of total node mass in this regime.

### B.4 Compressed Build (Float32 Regime)

Reduced-precision configuration:

- Embedding precision: Float32 (4 bytes/component)
- Structural topology unchanged

Embedding mass:

$$128 \cdot 4 = 512 \text{ bytes}$$

Structural linkage (optimized layout):

$$L \approx 120-150 \text{ bytes}$$

Metadata (compact encoding):

$$H \approx 20-60 \text{ bytes}$$

Total:

$$512 + (120-150) + (20-60) \approx 650-750 \text{ bytes}$$

Measured mean:

$$\approx 687 \text{ bytes per node}$$

## B.5 Generalized Density Expression

The governing density law remains:

$$\text{NodeSize} = d \cdot p + L + H$$

Where:

- $d \cdot p$  dominates total mass
- $L$  remains bounded by mean graph degree
- $H$  remains bounded by encoding design

Thus, scaling is precision-governed, not topology-governed.

## B.6 Clarification of Regimes

Regime	Precision	Measured Node Size
High-Precision Baseline	Float64	~1.3 KB
Compressed Build	Float32	~687 B

These are distinct precision configurations of the same deterministic substrate. They are not conflicting measurements.

## B.7 Role in Capacity Scaling

The density derivation directly supports Section 5:

- Storage scaling is determined by per-node byte mass
- Compute cost was shown independent of total cardinality (Section 4)
- Therefore scaling limit becomes a memory-envelope constraint

This appendix formalizes the byte-level foundation of that claim.

## Appendix C, Quantization Envelope

*This appendix formalizes the precision-scaling envelope implied by the density dominance of embedding mass.*

Precision	Bytes/ Component	Embedding Mass	Estimated Node Size	Nodes per 1 TiB
Float64	8	1024 B	~1.3 KB	~0.8B
Float32	4	512 B	~687 B	~1.6B
Float16	2	256 B	~450–600 B	>2B
Int8	1	128 B	~300–400 B	>2.5B

As established in Appendix B, per-node size is governed by:

$$\text{NodeSize} = d \cdot p + L + H$$

where:

- $d$  = embedding dimension
- $p$  = bytes per component
- $L$  = bounded structural linkage overhead
- $H$  = bounded metadata overhead

Because  $d \cdot p$  dominates total node mass, precision selection becomes the primary scaling lever.

### C.1 Precision as Scaling Parameter

For fixed embedding dimension  $d = 128$ , reducing component precision reduces node mass linearly:

- Float64  $\rightarrow$  8 bytes/component
- Float32  $\rightarrow$  4 bytes/component
- Float16  $\rightarrow$  2 bytes/component
- Int8  $\rightarrow$  1 byte/component

Structural linkage  $L$  and metadata  $H$  remain bounded and largely independent of precision.

Thus:

$$\text{NodeSize}(p) \approx 128 \cdot p + L + H$$

Embedding quantization directly compresses total memory footprint without altering graph topology or traversal mechanics.

## C.2 Measured vs. Projected Regimes

Measured regimes:

- Float64 (~1.3 KB/node)
- Float32 (~687 B/node)

Projected regimes:

- Float16
- Int8

Projected regimes derive strictly from embedding mass reduction under fixed topology. They do not alter:

- Traversal mechanics
- Operator locality
- Structural boundedness
- Compute invariance properties

They represent storage-density projections only.

## C.3 Scaling Implication

Because structural overhead is bounded and traversal is local, quantization modifies memory capacity limits without changing computational scaling behavior.

This preserves the bounded-local constraint:

$$\text{Work}(g(t), \Delta s) \leq K, \quad K \perp M$$

Therefore:

- Precision affects maximum addressable node count within a fixed memory envelope.
- Precision does not alter the governing scaling law of compute.

## Appendix D, Disclosure Boundary

This appendix defines the implementation boundary of the present work under active provisional and pending filings. Its purpose is to distinguish between:

- Formally described structure
- Empirically measured behavior
- Constructive implementation details intentionally withheld

The goal is transparency of scope without disclosure of proprietary mechanisms.

### D.1 Publicly Described Components

The following elements are fully described within this paper:

1. Deterministic Evolution Operator  $g(t)$ 
  - Time-modulated state evolution
  - Bounded-local traversal
  - Finite neighborhood constraint
  - No global recomposition
2. Structural Guarantees
  - Work bounded independently of total memory cardinality
  - No global scan during traversal
  - No similarity-sweep retrieval
  - No probabilistic re-inference during steady-state operation
3. Empirical Measurements
  - Traversal latency invariance (up to 25M nodes)
  - CPU utilization invariance
  - Absence of scale-correlated thermal signature
  - Per-node density under defined precision regimes

These components are sufficient for independent evaluation of the system's scaling claims.

### D.2 Withheld Implementation Details

The following elements are intentionally abstracted:

- Internal construction of the Magnitude Suppression Operator  $\Phi_t$
- Specific operator optimization strategies
- Memory layout optimizations beyond those required for density accounting
- Low-level mutation scheduling strategies
- Certain internal guard conditions related to structural invariants

These omissions do not affect the verifiability of the scaling law, density derivation, or measured invariants reported in the main text.

They pertain to constructive implementation details rather than to the formal or empirical claims.

---

### D.3 Auditability Boundary

The paper provides:

- A formal mathematical lineage (Appendix A)
- Explicit density accounting (Appendix B)
- Quantization envelope projections (Appendix C)
- Empirical scaling invariants (Section 4)

This structure permits architectural audit at the level of:

- Scaling law validity
- Thermodynamic behavior
- Storage-density realism
- Deterministic locality constraints

While reserving implementation-specific mechanisms under existing filings.

### D.4 Scope Clarification

This work claims:

- Existence of a bounded-local deterministic semantic substrate
- Empirical confirmation of compute invariance under measured regimes
- Capacity-bound scaling under defined memory envelopes

It does not disclose:

- Complete operator construction
- Full optimization stack
- All internal structural constraints

The distinction preserves intellectual property while maintaining scientific clarity.

## Appendix E — Scaling Boundaries and Validation Scope

*This appendix clarifies the scope and assumptions underlying the scaling argument presented in Section 5.*

### E.1 Validated Regime

Empirical invariance (Sections 4.2–4.4) was demonstrated under the following conditions:

- Node counts up to 25M
- Stable mean degree ( $\mu \approx 9.96$  edges/node)
- Local traversal bounded to finite neighborhoods
- Continuous steady-state operation

Traversal latency, CPU utilization, and thermal behavior remained invariant across a  $25\times$  increase in graph cardinality (1M  $\rightarrow$  25M).

No empirical measurements were conducted beyond 25M nodes.

### E.2 Capacity Projection Scope

The 1.6B node figure presented in Section 5 is derived from:

- Empirically measured per-node density (Section 4.5)
- Binary memory accounting
- A fixed 1 TiB memory envelope

It is therefore a capacity-bound projection, not a measured runtime regime.

No claim is made that traversal invariance has been experimentally validated at billion-node scale.

### E.3 Bounded-Local Assumption

The scaling argument relies on the bounded-local evolution constraint:

$$\text{Work}(g(t), \Delta s) \leq K, \quad K \perp M$$

This assumes:

- Degree distribution remains bounded
- Traversal remains locality-preserving
- No adversarial densification occurs
- No global mutation patterns dominate steady-state operation

Worst-case global rewrites fall outside the steady-state semantic evolution regime characterized in this work.

## E.4 Memory Hierarchy Considerations

Measurements were conducted under working-set conditions consistent with the tested scale regime.

The present work does not characterize:

- DRAM bandwidth saturation effects at billion-node scale
- NUMA or distributed memory behavior
- Extreme tail-latency under adversarial access patterns

Such evaluation remains future work.

## E.5 Thermodynamic Framing

Thermal invariance was measured via:

- Stable CPU utilization
- Absence of scale-correlated thermal ramp

Direct joule-level energy instrumentation was not performed.

Thermodynamic interpretation follows from bounded-local work and observed absence of scale-correlated escalation within the tested regime.

## Appendix F — Cache Locality and Memory Access Patterns

One common failure mode in large-scale graph systems is pointer-chasing inefficiency, where traversal becomes limited by cache misses rather than algorithmic complexity.

OPAL mitigates this through contiguous memory layouts and deterministic indexing.

### Structural Layout

Nodes and adjacency structures are stored using CSR-style contiguous arrays:

```
node_table[ ]
edge_offsets[ ]
edge_targets[ ]
```

Traversal therefore resolves as:

node → edge\_offsets[node] → contiguous edge\_targets range

This reduces:

- random memory access
- pointer indirection
- branch misprediction

Because adjacency lists are contiguous, the CPU can prefetch neighbor data efficiently.

### Node Memory Accounting

Each OPAL node is represented as a compact binary structure designed to balance semantic density with predictable memory access.

Example node composition:

<b>Vector</b>	encoding	256	<i>bytes</i>
<b>Topolog</b>	y metadata	96	<i>bytes</i>
<b>Semanti</b>	c tags	128	<i>bytes</i>
<b>Invaria</b>	nt storage	128	<i>bytes</i>
<b>Index r</b>	eference	79	<i>bytes</i>
<b>Total</b>		687	<i>bytes</i>

This fixed-size node representation allows deterministic addressing and improves cache predictability during traversal operations.

## Observed Behavior

During benchmark runs up to 25M nodes, the system exhibited:

- table CPU utilization (~17.2%)
- no thermal drift
- constant traversal latency (~0.32 ms mean)

This indicates that traversal operations remained cache-friendly and did not saturate the memory bus.

The primary scaling constraint encountered during testing was DRAM capacity, not compute throughput.

## Appendix G — Deterministic State vs Probabilistic Inference

A frequent misunderstanding is that OPAL attempts to replace probabilistic models.

This is not the case.

OPAL instead separates the AI architecture into two operational layers.

Layer	Role
Deterministic substrate	persistent semantic state
Probabilistic models	interpretation, generation

### Deterministic Substrate

The OPAL substrate provides:

- persistent node identity
- deterministic recall
- stable semantic topology

This eliminates the need for repeated embedding reconstruction or context window rehydration.

### Probabilistic Models

Stochastic models remain responsible for:

- natural language interpretation
- ambiguity resolution
- generative reasoning

In this configuration, probabilistic models operate on stable semantic structures rather than reconstructing context each time.

The result is a hybrid system where:

memory = deterministic  
reasoning = probabilistic

## Appendix H — Degree Growth and Structural Stability

Graph complexity in OPAL is determined by the neighborhood degree ( $D$ ).

$$T_{update} = O(D)$$

Where:

$D$  = number of connected neighbors

$N$  = total nodes

Because traversal operates only on the local adjacency neighborhood of the active node, the computational work required for a traversal step remains independent of the total memory dimension  $M$  when locality constraints are satisfied.

### API Degree Control

The architecture exposes degree constraints through the API.

Application designers may:

1. Bound  $D$  for strict constant-time updates.
2. Allow unbounded  $D$  for richer semantic connectivity.

This flexibility allows the substrate to be tuned for different workloads.

### Vector Security Layer

To protect the graph when  $D$  grows large, OPAL introduces a repair mechanism.

The Vector Security layer performs probabilistic reconstruction of corrupted nodes by evaluating neighboring vector relationships.

If a node invariant becomes invalid:

Neighbor relationships are sampled.

Statistical weighting estimates the missing invariant.

The node is re-integrated into the topology.

This prevents cascading structural failures even when the graph becomes highly connected.

The system also exposes degree and constraint controls through the API, allowing implementers to bound graph connectivity when stricter structural guarantees are required.

## Appendix I — System Scaling Considerations

The OPAL | ONE prototype has demonstrated deterministic traversal stability up to 25 million nodes on consumer Apple Silicon hardware. At this scale the limiting factor encountered during benchmarking was DRAM capacity rather than compute throughput or traversal efficiency.

The observations below clarify how the substrate is expected to behave as deployments extend beyond the experimental environment.

### I.1 Cache Behavior Beyond 25M Nodes

Benchmark runs remained thermodynamically stable through the tested regime, exhibiting constant traversal latency (~0.32 ms mean) and stable CPU utilization (~17.2%). The contiguous CSR-style memory layout used by the substrate ensures predictable access patterns that remain compatible with modern CPU prefetch mechanisms.

As graph size grows beyond the current experimental boundary, traversal performance is expected to track memory bandwidth and cache-prefetch characteristics rather than algorithmic complexity. Because adjacency lists are stored contiguously, the traversal path maintains sequential memory access properties that minimize pointer chasing and branch misprediction.

The primary constraint observed in testing was system memory capacity, indicating that the substrate remains compute-efficient within the tested regime.

### I.2 Multi-Socket and Distributed Deployment

The OPAL substrate is deterministic with respect to node identity and traversal semantics, allowing the graph to be partitioned without altering local traversal behavior. In multi-socket or distributed environments, node identity ranges can be deterministically assigned to independent substrate segments while preserving traversal invariants within each shard. Because recall operations follow explicit topology rather than probabilistic reconstruction, cross-shard interaction occurs only when graph edges span partition boundaries.

This allows distributed deployments to treat the substrate as a set of deterministic graph partitions rather than a probabilistic retrieval index. As a result, distribution becomes a systems-engineering concern rather than an algorithmic limitation of the substrate itself.

### I.3 Write Throughput Characteristics

OPAL employs a unified write/recall path in which encoding and traversal operate on the same structural topology.

Node insertion therefore follows the same deterministic traversal mechanics used during recall. Because the encoding process resolves directly to node identity and adjacency relationships, insertion does not require secondary indexing or embedding reconstruction. This architectural symmetry eliminates the traditional separation between write pipelines and recall pipelines present in many memory systems.

Throughput characteristics are therefore governed primarily by memory bandwidth and graph degree rather than global graph size.

#### **I.4 Mutation and Update Behavior**

Graph updates occur locally within the adjacency neighborhood of the affected node.

Update complexity scales with local node degree  $O(D)$ , where  $D$  represents the number of adjacent edges participating in the mutation operation. When degree bounds are applied through the API control layer, update cost becomes constant with respect to total graph size. Because updates modify only local adjacency segments, structural changes do not require global graph reorganization.

The probabilistic repair layer further ensures that localized corruption or partial failure does not propagate into cascading structural instability across the substrate.

Together, these properties indicate that the OPAL architecture maintains deterministic traversal behavior while scaling along standard hardware boundaries such as memory capacity and bandwidth rather than algorithmic growth in graph size.